Clays and Clay Minerals, Vol. 48, No. 3, 322–330, 2000.

IRON-OXIDE MINERALOGY OF A MOLLISOL FROM ARGENTINA: A STUDY BY SELECTIVE-DISSOLUTION TECHNIQUES, X-RAY DIFFRACTION, AND MÖSSBAUER SPECTROSCOPY

SILVIA G. ACEBAL,[1] ANA MIJOVILOVICH,[2] ELSA H. RUEDA,[1] MARÍA E. AGUIRRE,[3] AND CELIA SARAGOVI[2]

[1]Departamento de Química e Ingeniería Química, Universidad Nacional del Sur, Av. Alem 1253, 8000 - Bahía Blanca, Argentina

[2]Departamento de Física, Comisión Nacional de Energía Atómica, Avda. Libertador 8250, 1429 - Buenos Aires, Argentina

[3]Departamento de Agronomía, Universidad Nacional del Sur, Altos del Palihue, 8000 - Bahía Blanca, Argentina

Abstract—Selective-dissolution techniques by ammonium oxalate (OX), dithionite-citrate-bicarbonate (DCB), and dithionite-ethylenediaminetetraacetic acid (D-EDTA), and X-ray diffraction and Mössbauer spectroscopy were used to identify and characterize iron oxides and oxyhydroxides in the <2-mm, <50-μm, and <2-μm size fractions of a Mollisol from Bahía Blanca, Argentina. Iron compounds are present at low concentrations in mixtures with quartz, Na-rich feldspar, illite, interstratified illite-montmorillonite, and traces of kaolinite. Total Fe and Al content increases as soil particle size decreases, from 4.3 and 13.3 wt. % in the <2-mm size fraction to 8.5 and 22.8 wt. % in the clay fraction (<2 μm), respectively. No more than 25–30% of the total Fe is associated with the crystalline and the amorphous Fe oxides. Weakly ferromagnetic hematite and goethite were identified in the different fractions. These phases have small particle sizes and/or low crystallinity. They may also have Al for Fe substitutions. Crystalline magnetite or maghemite is rare. These Fe-rich phases are probably coating coarser particles.

The efficiency of Fe removal is highest for the D-EDTA treatment and least efficient for the OX method, for all fractions. The opposite is true for Al removal. Poorly crystalline hematite and goethite, which are soluble in oxalate, are only present in the coarser fractions. Poorly crystalline and crystalline hematite and goethite, which are soluble in DCB and EDTA, are present in coarser fractions, but do not occur in the clay fraction. DCB treatment probably dissolves Al in the 2:1 type phyllosilicates occurring in this soil, whereas D-EDTA dissolves Fe in the hydroxy interlayers of the smectite minerals or in the silicate phases.

Key Words—Ammonium-Oxalate Dissolution Treatment, Chemical Analysis, Dithionite-Citrate-Bicarbonate Dissolution Treatment, Dithionite-Ethylenediaminetetraacetic Acid Dissolution Treatment, Mollisols, Mössbauer Spectroscopy, X-ray Diffraction.

INTRODUCTION

Iron oxides and other minerals, with portions of their structure having a variable charge, are major components in many acid soils, and these materials greatly affect soil adsorption. Soils from temperate regions have minerals which have a permanent charge rather than a variable charge on a portion of their structure and these minerals dominate. In these soils, many properties of soil adsorption are largely controlled by the metal oxides and oxyhydroxides present in the different soil fractions. In general, the amount of adsorption depends on surface area, chemical composition, cation-exchange capacity (CEC), and the degree of coating of the oxide or oxyhydroxide on the phyllosilicate present (Kinniburgh and Jackson, 1981).

Although these oxides and oxyhydroxide compounds have been extensively studied by numerous authors in different soil types (Gangas *et al.*, 1973; Kodama *et al.*, 1977; Bigham *et al.*, 1978; Campbell and Schwertmann, 1984; Vandenberghe *et al.*, 1986), there is little chemical and mineralogical data available on iron-oxide composition in Argentinian soils (Aguirre, 1987; Saragovi *et al.*, 1994; Mijovilovich, 1997; Mijovilovich *et al.*, 1998).

As a group, Mollisols occur in regions of high soil fertility and fair-to-adequate rainfall so that they probably comprise the world's most productive agricultural soil. The soil described in our study, a drier Mollisol, has weakly developed profiles (A_p, A_1, and AC horizons) with a solum thickness of 40 cm and a calcic typical horizon C_k.

Lack of aggregate stability, low amount of organic matter, and high content of silt and fine sand produces a structureless mass during drying, making cultivation difficult or impossible until the profile is re-wetted. This condition may be related to the presence of iron oxides and oxyhydroxides, because these soil components act to coat and bind agents among soil particles (Aguirre, 1987).

Selective-dissolution techniques, X-ray diffraction (XRD), and Mössbauer spectroscopy (MS) are commonly applied to identify soil iron oxides and oxyhydroxides. Iron oxides and oxyhydroxides may represent the smallest particle fraction present, and the crystallinity of these phases may be very poor. These characteristics demand very careful analysis involving sensitive techniques for mineral identification. Iron oxides showing poor crystallinity, for instance, yield

Table 1. Physico-chemical properties of the A_p horizon.

Parameter	Values
pH[1]	7.5
pH[2]	6.3
Organic matter (%)[3]	2.9
CEC ($cmol_c\ kg^{-1}$)[4]	30.4
Sand (%)[5]	41.5
Coarse silt (20–50 μm) (%)[5]	14.4
Fine silt (2–20 μm) (%)[5]	15.8
Clay (%)[5]	28.3
Specific surface area ($m^2\ g^{-1}$)[6]	69.87

[1] Measured in water suspension.
[2] Measured in 1 mol L^{-1} KCl 1:2.5 soil/solution ratio.
[3] Walkey (1946): OM method.
[4] Bower *et al.* (1952): CEC method.
[5] Robinson (1922): Pipette method.
[6] Carter *et al.* (1965): EGME method.

broad low-intensity XRD peaks, and these peaks sometimes overlap with high-intensity peaks from silicate minerals, thereby making identification and quantitative determination difficult.

In general, iron oxides are often concentrated in the fine clay fraction. However, in some soils from Argentina (Aguirre, 1987; Mijovilovich, 1997; Mijovilovich *et al.*, 1998) and Brazil (Allan *et al.*, 1988; Goulart, 1994) magnetic compounds are almost entirely found in the silt and sand fraction, thus making the study of these coarser fractions important.

This paper reports results obtained by XRD, MS, and selective chemical-dissolution techniques to study iron-oxide and oxyhydroxide mineralogy in an Argentinian soil. Iron-oxide mineralogy of this soil has not been previously studied in detail. Relevant data from all size fractions studied (<2 mm, <50 μm, and <2 μm) are presented.

MATERIALS AND METHODS

Samples

Surface soil samples (0–12 cm), representing the Ap horizon of a Petrocalcic Haplustoll from Bahía Blanca, Argentina, were used. Soil samples were air-dried, ground, and passed through a 2-mm stainless steel sieve to obtain the <2-mm size fraction; then ultrasonically dispersed in water and fractionated by standard sieve (50 μm) techniques to obtain the <50-μm size fraction. The clay fraction (<2 μm) was obtained by sedimentation techniques using Stoke's law (Robinson, 1922). Some physical and chemical properties of the soil are listed in Table 1.

Chemical analysis

Total soil, silt, and clay-fraction samples were treated with chemical extractants as described below, producing four subsamples for each fraction: (1) untreated (UT), (2) acid ammonium oxalate (OX) treated, (3) dithionite-citrate-bicarbonate (DCB) treated, and (4) dithionite-ethylenediaminetetraacetic acid (D-EDTA) treated. To extract poorly crystallized iron oxides, a single 2-h treatment in darkness with OX was performed (Schwertmann, 1964, 1973). For complete dissolution of all crystalline iron oxides and oxyhydroxides, the DCB procedure of Mehra and Jackson (1960) was performed four times sequentially using 1 g of sodium dithionite in hot (353 K) sodium citrate and sodium bicarbonate solution. The dissolving reagent D-EDTA was also used for dissolution of crystalline iron oxides (Rueda *et al.*, 1992). D-EDTA treatment was performed using 1 g of solid sodium dithionite, in a 0.05 mol dm^{-3}, pH 5.5 Na_2EDTA solution, under N_2 atmosphere at 315 K. Residues were washed free of excess salts and air-dried following each selective dissolution treatment.

Total iron and aluminum were determined after complete dissolution of soil fractions in a Pt crucible using the alkaline fusion method (Jackson, 1964). All treatments were performed in triplicate and Fe and Al contents in extracts were analyzed by atomic absorption spectroscopy (AAS).

X-ray diffraction

XRD studies were performed on each fraction, using CuKα (1.5406 Å) radiation (45 kV, 35 mA) on a Philips vertical goniometer in a range of $2° < 2\theta < 70°$. The diffractometer was equipped with a 1° divergence slit, a 0.1-mm receiving slit, and a monochromator. Analysis using Fe radiation gave no additional information. Additional patterns were obtained in the $2\theta = 20–35°$ range using CuKα radiation, a 0.01 2θ step, and a counting time of 5 s per 2θ increment.

The untreated clay fraction and residues from Mg saturation followed by glycerol solvatation, and K saturation followed by heating to 823 K (Jackson, 1979) were examined from $2\theta = 2–30°$ using a 0.01 step and a counting time of 30 s per 2θ increment, using the same equipment as above, at 36 kV, 18 mA, and without a monochromator and using a Ni filter. Residues from DCB and D-EDTA treatments, in powder form, were glycerol solvated, calcined at 823 K, and then similarly scanned.

Mössbauer spectroscopy

Mössbauer spectroscopy was performed on all samples at 300 and 15 K using a 25 mCi ^{57}Co source in a Rh matrix. In preparing the Mössbauer absorbers, special care was taken to use a "thin absorber" (Long *et al.*, 1983) and to eliminate "texture effects" (Ericsson and Wäppling, 1976). Reasonable fits using a Lorentzian-line shapes were obtained. A semiquantitative Mössbauer analysis of Fe-containing phases was performed by taking areas of subspectra as a measure for Fe compound concentrations (Muir, 1968).

All absorbers were prepared by grinding of the 12 samples in an agate mortar using ~8 mg/cm^2 of Fe.

https://doi.org/10.1346/CCMN.2000.0480303 Published online by Cambridge University Press

Table 2. Dissolution analysis (wt. %) of the soil fractions used in this study.

Fraction	[1]Fe_{ox}	Al_{ox}	[2]Fe_{DCB}	Al_{DCB}	[3]$Fe_{D\text{-}EDTA}$	$Al_{D\text{-}EDTA}$	[4]Fe_t	[4]Al_t
<2 mm	0.248	0.304	0.722	0.153	1.272	0.102	4.20	13.32
<50 μm	0.484	0.652	0.933	0.379	1.509	0.192	5.14	14.45
<2 μm	0.566	0.916	1.430	0.472	2.150	0.388	8.53	22.85

[1] OX: Oxalate-extractable Fe and Al.
[2] DCB: Dithionite-citrate-carbonate-extractable Fe and Al.
[3] D-EDTA: Dithionite-EDTA-extractable Fe and Al.
[4] Fe_t = total iron, Al_t = total aluminum.

Non-refined sugar was mixed with the samples to avoid preferred orientation of powder crystallites. Measurements using the magic angle were made to minimize texture effects. Coarser soil-sample fractions were further ground to obtain better homogeneity and to improve the reliability of area results (Saragovi and Mijovilovich, 1997). High counting rates ($3–5 \times 10^6$ counts/channel) were used, and a background correction was measured (Housley *et al.,* 1964). Similar experimental conditions were maintained for all measurements.

All spectra were fitted with the DIST3E program (Vandenberghe, 1992), which uses hyperfine parameter distributions. Two quadrupole doublet distributions (D1 and D2) and two hyperfine field distributions (S1 and S2) were employed and the goodness-of-fit of each distribution was determined by χ^2 criteria. The same range of values for the corresponding hyperfine parameters, hyperfine magnetic field (H), and quadrupole splitting (QS) was used for all samples in each distribution (S1, S2, D1, D2). When the temperature was lowered, these ranges were changed accordingly. For each subsample, relative populations of all four distributions were computed from the fitted areas. To compare results, areas of treated subsamples were normalized to the area of the corresponding untreated sample.

RESULTS

Chemical analysis

Chemical data of the different soil fractions are summarized in Table 2. Total iron and aluminum content increases as soil-particle size decreases. Substantial amounts of iron do not go into solution by treatment with DCB and D-EDTA. No more than 25–30% of the total iron is associated with crystalline and amorphous iron oxides and/or oxyhydroxides. Fe_{OX} values, accounting for <10% of total iron, indicate all samples contain small amounts of poorly crystallized oxalate-soluble Fe-oxides, magnetite, and maghemite. Fe_{OX}/Fe_{DCB} ($Fe_{OX/DCB}$) ratios vary between 0.34–0.52 indicating that better crystallized Fe-oxides are also present.

The amount of DCB-extracted aluminum is greater than for that obtained by D-EDTA extraction. Acid-oxalate-extractable Al (Al_{OX}) is greater than DCB-extractable Al (Al_{DCB}) and D-EDTA-extractable Al ($Al_{D\text{-}EDTA}$). The molar ratio Al/(Al + Fe) ranges from 0.11 (in <2-mm size soil fraction) to 0.22 (in <2-μm size clay fraction) mol mol^{-1}, according to the D-EDTA values (Table 2). These results suggest the presence of medium to high Al-substituted sites in the soil iron oxides (Cornell and Schwertmann, 1996).

X-ray diffraction analysis

Iron-oxyhydroxide identification was difficult owing to the low concentration and the overlap of reflections from other phases present in the soil, particularly quartz and feldspar. In the range of 2θ = 20–35°, Fe-oxides and oxyhydroxides secondary peaks do not overlap with peaks from other phases in the soil. The comparison of chemically treated and untreated samples allowed the identification of some iron oxides. Despite the use of the backfill method for preparing the sample, displacement of the 0.334-nm reflection of quartz (~0.05 nm) was observed, thereby making the application of differential XRD analysis difficult (Schulze, 1981; Campbell and Schwertmann, 1984, 1985).

In all samples, large amounts of quartz (0.427, 0.334 nm), Na-rich feldspar (0.405, 0.324, 0.321, 0.250 nm), and illite (1.000, 0.334 nm) were observed. The 0.334-nm peak was assigned mainly to quartz or Na-rich feldspar because no additional mica reflections occurred; no mica is present in this soil (Blanco and Sánchez, 1995).

X-ray diffractograms from the size fractions of <2 mm, <50 μm, and <2 μm for both treated and untreated subsamples are shown in Figures 1–3. For the size fractions of <50 μm, hematite and goethite were identified; goethite in minor amounts. The intensities of both hematite (0.269 and 0.368 nm) and goethite (0.421 and 0.269 nm) peaks decrease with chemical treatment. For patterns from the <2-mm size fraction, only the 0.269-nm reflection corresponds to hematite and minor amounts of goethite. In the untreated sample, the 0.329-nm reflection is assigned to lepidocrocite (intensity = 90%), but the absence of additional reflections, in particular the 0.626-nm reflection, makes this conclusion tentative. The possible presence of lepidocrocite is not consistent with the assumed en-

https://doi.org/10.1346/CCMN.2000.0480303 Published online by Cambridge University Press

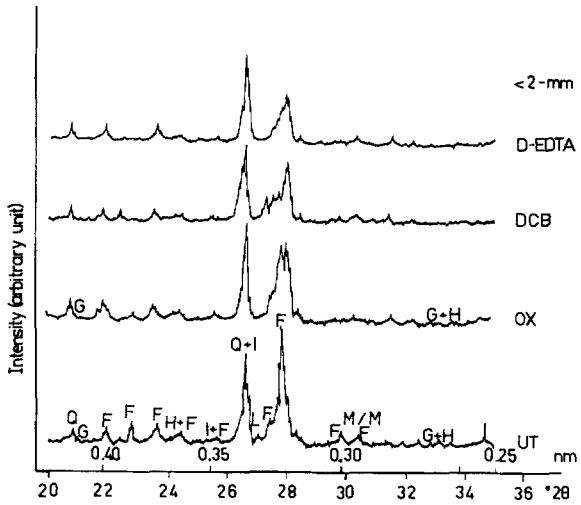

Figure 1. XRD patterns of <2-mm size soil fraction before treatment and following selective dissolution by OX, DCB, and D-EDTA treatments. G, goethite; L, lepidocrocite; H, hematite; M/M, maghemite/magnetite; I, illite; Q, quartz; F, Na-rich feldspar; K, Kaolinite; I-M, interstratified illite-montmorillonite.

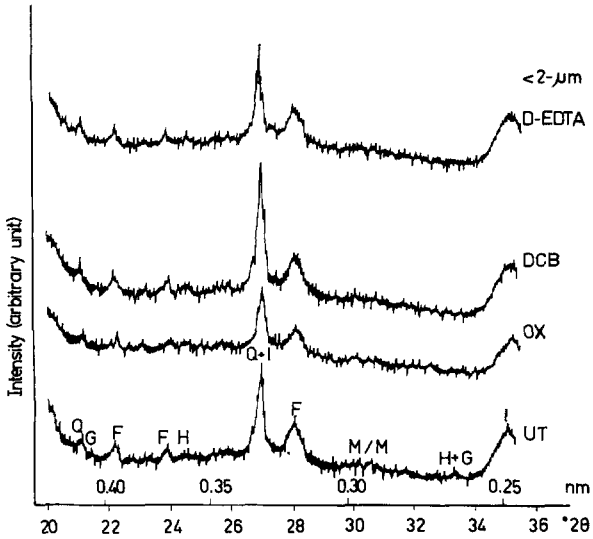

Figure 3. XRD patterns of <2-μm size clay fraction before treatment and following selective dissolution by OX, DCB, and D-EDTA treatments. Symbols as in Figure 1.

vironmental conditions of the soil (Aguirre, 1987; Acebal, 1989).

In the size fractions of <2 mm and <50 μm, the 0.297-nm reflection slightly decreased in intensity after the chemical treatments, suggesting the presence of maghemite and/or magnetite. If maghemite and/or magnetite are present, the most intense 0.253–0.251-nm peaks would overlap those corresponding to feldspar. For the <2-μm size fraction, patterns show the presence of goethite and hematite peaks. The 0.269-nm reflection is just noticeable in untreated soil; DCB and D-EDTA treatments remove this peak, causing a relative increase in the intensities of quartz and phyllosilicate peaks.

Diffractograms of untreated, glycerol-solvated, and calcined material from the <2-μm size fraction are shown in Figure 4. These patterns show the presence of poorly crystalline materials, such as expandable clays of the smectite group and randomly interstratified illite-montmorillonite (1.000–1.506 nm). In addition, illite (1.000 nm), traces of kaolinite (0.707 nm), and non-clay minerals such as quartz (0.334, 0.427 nm) and Na-rich feldspar (0.324, 0.321, 0.405, 0.640, 0.250 nm) are also present. Diffractograms from untreated clay, glycerol-solvated, and calcined samples

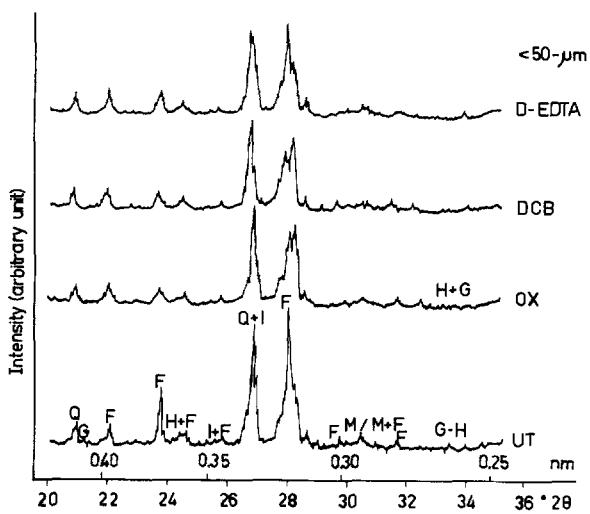

Figure 2. XRD patterns of <50-μm size soil fraction before treatment and following selective dissolution by OX, DCB, and D-EDTA treatments. Symbols as in Figure 1.

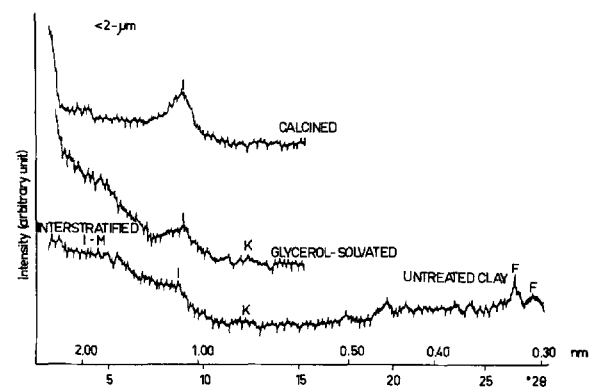

Figure 4. XRD patterns from the untreated clay fraction (<2 μm) and following glycerol solvation and calcination. Symbols as in Figure 1.

https://doi.org/10.1346/CCMN.2000.0480303 Published online by Cambridge University Press

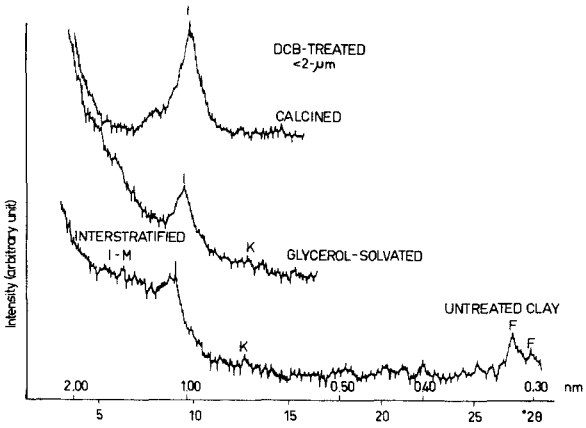

Figure 5. XRD patterns from the untreated clay fraction (<2 μm), and after glycerol solvation and calcination following dissolution by DCB treatment. Symbols as in Figure 1.

after DCB and D-EDTA treatments are shown in Figures 5 and 6.

Mössbauer spectroscopy

Characteristic Mössbauer spectra are shown in Figure 7. Figure 8 shows hyperfine field distributions corresponding to the fitted spectrum of the DCB treated <2-mm size fraction sample (Figure 7b). Fitted parameters at room temperature (RT) are presented in Table 3, where values of the maxima in the distribution profiles are expressed as H_M and QS_M. In cases where a distribution has several similar maxima, all are given. Isomer shift (IS) values are referred to α-Fe.

The paramagnetic doublets, D1 and D2, are caused by Fe^{3+} and Fe^{2+} ions, respectively, located in illite and/or in montmorillonite (Rozenson and Heller-Kallai, 1976; Coey, 1980; Murad and Wagner, 1994). A kaolinite contribution to the Fe^{3+} doublet is also possible. These quadrupolar distributions remain very similar in shape and range when temperature is low-

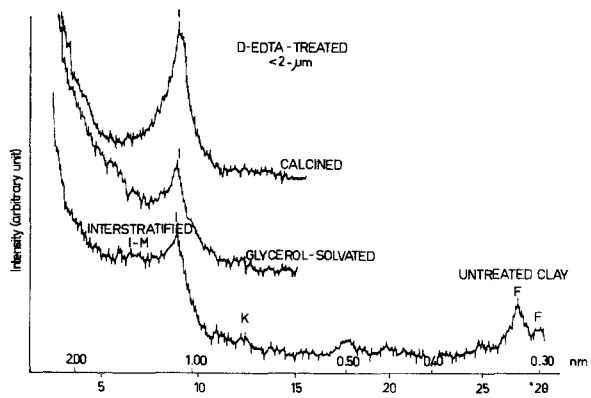

Figure 6. XRD patterns from the untreated clay fraction (<2 μm), and after glycerol solvation and calcination following dissolution by D-EDTA treatment. Symbols as in Figure 1.

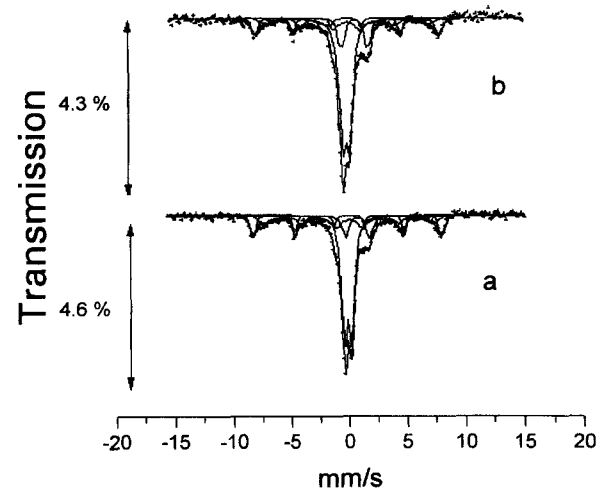

Figure 7. Room-temperature Mössbauer spectra of <2-mm size fraction a) untreated sample, b) DCB-treated sample.

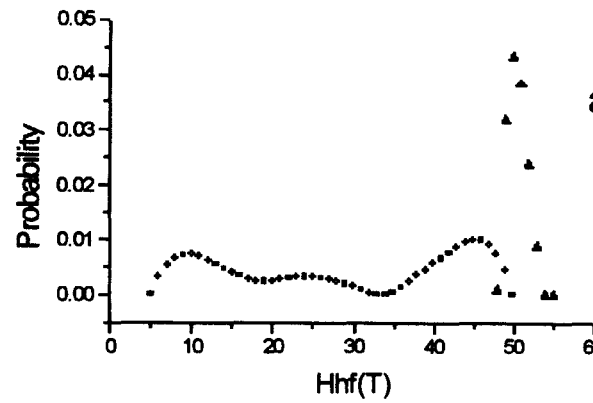

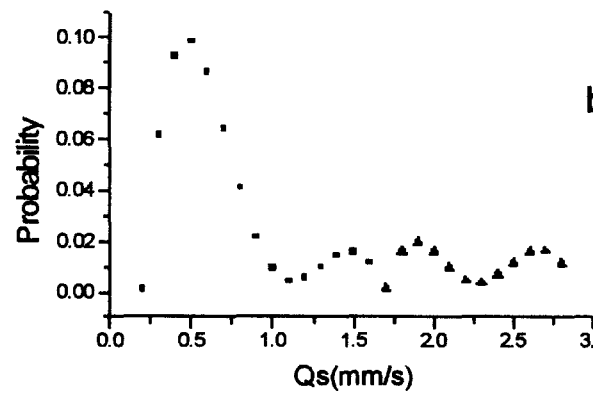

Figure 8. Hyperfine field distributions corresponding to Figure 7b. Symbols: ▲ = S1, ◆ = S2 in Figure 8a, and ■ = D1, ▲ = D2 in Figure 8b.

https://doi.org/10.1346/CCMN.2000.0480303 Published online by Cambridge University Press

Table 3. Room-temperature Mössbauer parameters. H values are in Tesla and QS and IS are in mm/s.

	S1			S2			D1		D2	
	H_M	QS	IS	H_M	QS	IS	QS_M	IS	QS_M	IS
				<2 mm						
Untreated	50.4	−0.17	0.30	9, 30, 46	−0.13	0.37	0.50	0.28	1.9, 2.7	1.12
OX-treated[1]	50.3	−0.10	0.26	9, 28, 46	−0.06	0.32	0.50	0.27	1.9, 2.7	1.09
DCB-treated[1]	50.2	−0.13	0.25	9, 24, 46	−0.18	0.28	0.50	0.28	1.9, 2.7	1.05
D-EDTA-treated[1]	50.0	−0.25	0.40	8, 30, 45	−0.24	0.48	0.50	0.38	2.0, 2.7	1.26
				<50 μm						
Untreated	50.0	−0.23	0.60	8, 32, 46	−0.11	0.57	0.50	0.45	1.9, 2.7	1.30
OX-treated	9, 31, 35, 50	−0.20	0.48	[2]#	#	#	0.50	0.46	1.9, 2.7	1.33
DCB-treated	9, 30, 50	−0.24	0.52	#	#	#	0.40	0.45	2.0, 2.7	1.38
D-EDTA-treated	50.0	−0.13	0.44	#	#	#	0.50	0.44	1.9, 2.7	1.34
				<2 μm						
Untreated	51.0	−0.21	0.41	8, 26, 47	−0.28	0.38	0.50	0.39	2.2	1.39
OX-treated	51.0	−0.24	0.41	9, 28, 47	−0.17	0.42	0.45	0.39	2.2	1.42
DCB-treated							0.50	0.39	2.6	1.18
D-EDTA-treated							0.50	0.30	1.9, 2.2	1.33

[1] OX-treated, DCB-treated, and D-EDTA-treated as in Table 2.
[2] Only one "S" distribution is used (see text).

ered, although QS2 shifts slightly to higher values. Low-temperature results do not suggest the presence of lepidocrocite and/or ferrihydrite, in agreement with XRD data.

The magnetic components of the spectra were fitted with two sextet distributions, S1 and S2 (Saragovi *et al.,* 1994). The S1 distribution is narrow, whereas S2 is a broad distribution. Hence, it is possible to model the observed sharp lines with broad shoulders, thus clarifying the assignments. The S1 parameters are assigned to Fe^{3+} ions in weakly ferromagnetic hematite (Vandenberghe *et al.,* 1990). When temperature is lowered, the H_M value shifts to 52 T, the QS value remains negative whereas the corresponding area does not increase. The negative QS value indicates that the Morin transition did not occur; this is consistent with the degree of substitution of Al for Fe (Murad and Schwertmann, 1986; Vandenberghe *et al.,* 1990).

For the broad distribution of S2, parameters are in agreement with goethite, magnetite and/or maghemite, and hematite (Bowen, 1979; Murad, 1979; Murad and Schwertmann, 1980; Bowen and Weed, 1984; Vandenberghe *et al.,* 1990). Higher magnetic fields suggest the presence of hematite and magnetite or maghemite; the hematite is probably highly substituted and/or has a small particle size (Mijovilovich, 1997). Traces of magnetite or maghemite were isolated by magnetic separation in the coarser fractions. The richest magnetic extract showed a negligible saturation magnetization value, 1.6 σ_s/JT^{-1} kg^{-1} (Mijovilovich, 1997; A. Mijovilovich, pers. comm., 1998). These results indicate that magnetite or maghemite contributions are negligible. Low magnetic fields (≤25 T) and an S2 distribution which becomes slightly narrower and shifts to higher cut-off values when temperature is lowered indicate the presence of goethite. Goethite has a varying degree of crystallinity and/or Al substitution, which makes its identification uncertain. In some cases, only one S distribution is sufficient to describe the spectra in which the peaks are broad. This S distribution supports the conclusion that the samples contain mostly poorly crystalline and/or medium to highly Al-substituted goethite.

As noted above, a semiquantitative analysis of Fe-bearing compounds is possible by taking subspectral areas as proportional to concentrations. This analysis allows the observation of selectivity and specificity trends of chemical treatments used. The i^{th} recoilless fraction values (f_i) were not considered because the same sample was analyzed by different treatments. Note that in all samples, the background correction value found was ~1.3. Table 4 shows the subspectral areas and the total areas for each particle size relative to the untreated sample area of the same size.

DISCUSSION

Hematite and goethite occur in this Mollisol, with varying degrees of crystallinity and Al substitution. Non-antiferromagnetic hematite and poorly crystalline and medium to highly Al-substituted goethite are present. Magnetite or maghemite is negligible. Illite and interstratified illite-montmorillonite are present.

Variations in Al_{OX} values (Table 2) are possibly related to the ability of acid-oxalate to dissolve certain poorly crystallized minerals with short-range order. (Jeanroy, 1983; Parfitt and Childs, 1988). Al_{DCB} values may reflect the ability of the DCB method to dissolve greater amounts of Al, as noted by Ryan and Gschwend (1991) for kaolinite and nontronite samples. Dissolution of aluminum hydroxy interlayers must also be considered.

https://doi.org/10.1346/CCMN.2000.0480303 Published online by Cambridge University Press

Table 4. Relative normalized areas in % from room temperature calculations.

Sample	S1[1] Narrow sextet	S2[1] Broad sextet	D1[1] Fe^{3+}	D2[1] Fe^{2+}	Total Fe
		<2 mm			
Untreated	15	23	51	11	100
OX-treated[2]	13	17	50	12	92
DCB-treated[2]	12	16	44	11	83
D-EDTA-treated[2]	9	11	30	14	64
		<50 μm			
Untreated	12	17	63	8	100
OX-treated	20	[3]#	53	8	81
DCB-treated	21	#	46	8	75
D-EDTA-treated	9	#	51	8	68
		<2 μm			
Untreated	4	12	79	5	100
OX-treated	5	12	75	4	96
DCB-treated			76	8	84
D-EDTA-treated			70	5	75

[1] Assignments (see text): S1 = Weakly ferromagnetic hematite; S2 = mainly goethite + WF hematite; D1 and D2 = paramagnetic Fe^{3+} and Fe^{2+}, respectively.

[2] UT = untreated, OX-treated, DCB-treated, and D-EDTA-treated as in Table 2.

[3] Only one "S" distribution is used (see text).

$Fe_{D\text{-}EDTA}$ values show that this method is more effective than the traditional DCB method for removing Fe. This result may be related to the use of a lower temperature and a N_2 atmosphere, which may prevent the decomposition of the reductant agent. Apparently, the iron, which is not brought into solution by DCB and D-EDTA, occurs either in a silicate phase or as an interlayer constituent of the hydroxy-interlayered 2:1 type minerals (*e.g.,* smectite, illite-smectite).

The calcined sample (Figure 4) did not show phases with 1.0-nm peaks typical of smectite, which may be related to the presence of Al (or Fe) hydroxy-interlayer material. In contrast, in the DCB-treated sample (Figure 5), the calcination produces phases with layers of 1.0 nm, suggesting that the DCB treatment removed interlayer material as was also reported by Jackson (1979). However, D-EDTA treatment did not apparently remove this hydroxy interlayer material (note the lack of 1.0-nm peaks that would suggest collapse in Figure 6). These observations are consistent with the chemical data of the <2-μm size fraction which show that the DCB treatment extracts more Al than the D-EDTA treatment. Comparison of XRD patterns (Figures 4–6) with values of Fe content derived from chemical treatment (Table 2) suggests that the D-EDTA treatment is both more effective and selective over DCB to dissolve crystalline iron oxides. The D-EDTA method is marginally more effective at removing iron-hydroxy interlayer structures over the DCB method.

The total-area values (Table 4) show an increase in the Fe-extraction rate with OX, DCB, and D-EDTA treatments, respectively. OX treatment removed the least of the iron compounds with efficiency increasing with DCB and D-EDTA. This trend is independent of the fraction considered, although the extracted amount varies in each fraction. In the <2-mm size fraction, values are near 10, 20, and 40%, respectively, and in the <2-μm size fraction, the values are ~5, 15, and 25%. Chemical analysis and MS results show that the obtained Fe_{OX}/Fe_t, Fe_{DCB}/Fe_t, and $Fe_{D\text{-}EDTA}/Fe_t$ ratios present similar trends in all fractions. Some differences are noted with OX owing to the error involved in the determination of small quantities.

OX decreases the S2 signals in coarser fractions (Table 4), whereas OX treatment does not appreciably affect the clay fraction (<2 μm). DCB and especially the D-EDTA method also decreases the S1 and S2 signals, but these treatments suppress the magnetic signal from the <2-μm size fraction. On the basis of these results and the assignments given above, the following is concluded: (1) OX extracts some of the poorly crystallized, small-sized, and/or Al-substituted hematite and goethite (on the basis of the S2 signal). (2) DCB and D-EDTA extract the small-sized and/or poorly crystallized and Al-substituted hematite and goethite (S2 signal). (3) DCB and D-EDTA extract hematite which is less well crystallized and medium Al-substituted (S1 signal). (4) D-EDTA is the most efficient. Hematite with either no Al content or low Al content is not present.

Chemical-treatment efficiency to extract soil iron compounds is known to increase as particle size decreases (Cornell and Schwertmann, 1996). Table 4 shows that the efficiency of these chemical treatments does not change drastically above the clay-size fraction. Note that for the clay fraction, DCB and D-EDTA eliminated the S1 and S2 signals. For the UT samples, the S1 and S2 signals decreased with sieving (*e.g.,* a reduction in grain size) which suggests that some oxides adhere to larger particles. Amorphous oxides (*i.e.,* poor crystallinity and/or very small grain size) and Al-substituted goethite and hematite extracted by the OX method are apparently present in coarser fractions. Coarser grain-size fractions contain both amorphous and crystalline iron oxides that are extracted by the DCB and D-EDTA methods. However, amorphous and crystalline iron oxides do not occur in the clay fraction.

These results suggest that weakly ferromagnetic hematite and goethite are probably adhering to coarse particles as a coating, in agreement with previous observations (Aguirre, 1987). Although the grain sizes of these oxides and oxyhydroxides are small, they are not sufficiently small to show superparamagnetic behavior as indicated by the 15 K spectra. Hematites of

<30-nm grain size should show superparamagnetic behavior.

Note (Table 4) that the S1 and S2 signals indicate that Fe^{3+} was extracted from the sample and the paramagnetic D1 signal indicates this to a lesser extent; the D1 signal decreases in all fractions, although this effect is more apparent after D-EDTA treatment. Since superparamagnetic oxides do not occur at temperatures as low as 15 K, this extracted paramagnetic Fe^{3+} must originate in clay minerals. The methods of DCB and, in particular, D-EDTA may be removing Fe from silicate phases (including the clays) or minerals with hydroxy interlayers. The lack of collapse of the smectite after D-EDTA treatment (Figure 6) indicates that the presence of Al is predominant over Fe in the hydroxy-interlayer material. The possibility of the presence of very low crystallinity and/or highly Al-substituted Fe oxides can not be discarded because such phases may be detected if temperatures <15 K were used in the MS experiments. On the basis of the D2 doublet, there is little Fe^{2+} and it is not affected appreciably by chemical treatment.

ACKNOWLEDGMENTS

AM acknowledges valuable discussion with M. Benyacar (CNEA, Argentina), and CS is indebted to CONICET, Argentina.

REFERENCES

Acebal, S.G. (1989) Comportamiento de algunas sustancias complejantes como agentes de extracción de elementos menores en suelos. Ph.D. thesis, Universidad Nacional del Sur, Bahia Blanca, Argentina, 170 pp.

Aguirre, M.E. (1987) Rol de los minerales amorfos en el proceso de cementación a la agregación. MS. thesis, Universidad Nacional del Sur, Bahia Blanca, Argentina, 157 pp.

Allan, J.E.M., Coey, J.M.D., Resende, M., and Fabris, J.D. (1988) Magnetic properties of iron-rich oxisols. *Physical Chemistry Mineralogy,* **15,** 470–475.

Bigham, J.M., Golden, D.C., Bowen, L.H., Buol, S.W., and Weed, S.B. (1978) Iron oxide mineralogy of well-drained Ultisols and Oxisols: I. Characterization of iron oxides in soil clays by Mössbauer spectroscopy, X-ray diffractometry, and selected chemical techniques. *Soil Science Society of America Journal,* **42,** 816–825.

Blanco, M.C. and Sánchez, L.F. (1995) Caracterización de las fracciones limo y arcilla en suelos loésicos del suroeste pampeano en Argentina. *Turrialba,* **45,** 76–84.

Bowen, L.H. (1979) Mössbauer spectroscopy of ferric oxide and hydroxides. *Mössbauer Effect Reference Data Journal,* **2,** 76–94.

Bowen, L.H. and Weed, S.B. (1984) Mössbauer spectroscopy of soils and sediments. In *Chemical Mössbauer Spectroscopy,* R.H. Herber, ed., Plenum Publishing Corp., New York, 217–242.

Bower, C.A., Reitemeier, R.F., and Fireman, M. (1952). Exchangeable cation analysis of saline and alkali soils. *Soil Science,* **73,** 251–253.

Campbell, A.S. and Schwertmann, U. (1984) Iron oxide mineralogy of placic horizons. *Journal of Soil Science,* **53,** 569–582.

Campbell, A.S. and Schwertmann, U. (1985) Evaluation of selective dissolution extractants in soil chemistry and mineralogy by differential X-ray diffraction. *Clay Minerals,* **20,** 515–519.

Carter, D.L., Heilman, M.D., and González, C.L. (1965) Ethylene glycol monoethyl ether for determining surface area of silicate minerals. *Soil Science,* **100,** 356–360.

Coey, J.M.D. (1980) Clay minerals and their transformations studied by nuclear techniques. *Atomic Energy Review,* **18,** 73–124.

Cornell, R.M. and Schwertmann, U. (1996). *The Iron Oxides.* VCH Publishers, Weinheim, 573 pp.

Ericsson, T. and Wäppling, R. (1976) Texture effects in 3/2-1/2 Mössbauer spectra. *Journal de Physique,* **6,** 719–723.

Gangas, N.H., Simopoulos, A., Kostikas, A., Yassoglou, N.J., and Filippakis, S. (1973) Mössbauer studies of small particles of iron oxides in soils. *Clays and Clay Minerals,* **21,** 151–160.

Goulart, A.T. (1994). Propiedades estructurais e magnéticas de óxidos de ferro presentes em solos magnéticos oriundos de basalto e tufitos. Ph.D. thesis, Universidade Federal de Minas Gerais, Belo Horizonte, Brazil, 124 pp.

Housley, R.M., Erickson, N.E., and Nash, J.D. (1964). Measurement of recoil-free fractions in studies of the Mössbauer efect. *Nuclear Instrument Methods,* **27,** 29–37.

Jackson, M.L. (1964) *Análisis Qulmico de Suelos.* Ediciones Omega, Barcelona, 368–440.

Jackson, M.L. (1979) *Soil Chemical Analysis—Advanced Course, 2nd edition.* Published by the author, Madison, Wisconsin, 895 pp.

Jeanroy, E., Guillet, B., Delcroix, P., and Janot, Ch. (1983) Les formes du fer dans les sols: Confrontation des méthodes chimiques avec la spectrométrie Mössbauer. *Science du Sol,* **3–4,** 185–194.

Kinniburg, D.G. and Jackson, M.L. (1981) Cation adsorption by hydrous metal oxides and clay. In *Adsorption of Inorganics at Solid—Liquid Interfaces,* M.A. Anderson and A.J. Rubin, eds., Ann Arbor Science Publishers, Ann Arbor, Michigan, 91–160.

Kodama, H., McKeague, J.A., Tremblay, R.J., Gosselin, J.R., and Townsend, M.G. (1977) Characterization of iron oxide compounds in soils by Mössbauer and other methods. *Canadian Journal of Earth Science,* **14,** 1–15.

Long, G.J., Cranshaw, T.E., and Longworth, G. (1983) The ideal Mössbauer effect absorber thicknesses. *Mössbauer Effect Data Reference Journal,* **6,** 42–49.

Mehra, O.P. and Jackson, M.L. (1960) Iron oxide removal from soils and clays by a dithionite-citrate system buffered with sodium bicarbonate. *Clays and Clay Minerals,* **7,** 317–327.

Mijovilovich, A. (1997) Estudio Mössbauer de óxidos e hidróxidos de Fe: Aplicación al estudio de suelos. Ph.D. thesis, Universidad Nacional de Buenos Aires, Buenos Aires, Argentina, 88 pp.

Mijovilovich, A., Morrás, H., Saragovi, C., Santana, G., and Fabris, J.D. (1998) Magnetic fraction from an Ultisol from Misiones, Argentina. *Hyperfine Interactions C,* **3,** 332–335.

Muir, A.H. (1968) Analysis of complex Mössbauer spectra by stripping techniques. In *Mössbauer Effect Methodology, Volume 4,* I.J. Gruverman, ed., Plenum Press, New York, 75–101.

Murad, E. (1979) Mössbauer and X-ray data on β-FeOOH (akaganeite). *Clay Minerals,* **14,** 273–283.

Murad, E. and Schwertmann, U. (1980) The Mössbauer spectrum of ferrihydrite and its relations to those of other iron oxides. *American Mineralogist,* **65,** 1044–1049.

Murad, E. and Schwertmann, U. (1986) Influence of Al substitution and crystal size on the room-temperature Mössbauer spectrum of hematite. *Clays and Clay Minerals,* **34,** 1–6.

Murad, E. and Wagner, U. (1994) The Mössbauer spectrum of illite. *Clay Minerals,* **29,** 1–10.

Parfitt, R.L. and Childs, C.W. (1988) Estimation of forms of Fe and Al: A review, and analysis of contrasting soils by dissolution and Mössbauer methods. *Australian Journal of Soil Research,* **26,** 121–144.

Robinson, G.W. (1922) A new method for the mechanical analysis of soils and other dispersions. *Journal of Agricultural Science,* **12,** 306–321.

Rozenson, I. and Heller-Kallai, L. (1976) Reduction and oxidation of Fe^{3+} in dioctahedral smectites I: Reduction with hydrazine and dithionite. *Clays and Clay Minerals,* **24,** 271–282.

Rueda, E.H., Ballesteros, M.C., Grassi, R.L., and Blesa, M.A. (1992) Dithionite as a dissolving reagent for goethite in the presence of EDTA and citrate. Application to soil analysis. *Clays and Clay Minerals,* **40,** 575–585.

Ryan, J.N. and Gschwend, P.M. (1991) Extraction of iron oxides from sediments using reductive dissolution by titanium (III). *Clays and Clay Minerals,* **39,** 509–518.

Saragovi, C. and Mijovilovich, A. (1997) A warning on the use of Mössbauer spectroscopy in semiquantitative analysis of soils. *Clays and Clay Minerals,* **45,** 480–482.

Saragovi, C., Labenski, F., Duhalde, S.M., Acebal, S.G., and Venegas, R. (1994) Mössbauer studies on some Argentinian soil: Mollisols from Bahía Blanca. *Hyperfine Interactions,* **91,** 765–769.

Schulze, D.G. (1981) Identification of soil iron oxides minerals by differential X-ray diffraction. *Soil Science Society of America Journal,* **45,** 437–440.

Schwertmann, U. (1964) Differenzierung der Eisenoxide des Bodens durch photochemische Extraktion mit saurer Ammoniumoxalat-Lösung. *Zeitschritt Pflanzenemährung Düngung und Bodenkunde,* **105,** 194–202.

Schwertmann, U. (1973) Use of oxalate for Fe extraction from soils. *Canadian Journal of Soil Science,* **53,** 244–246.

Vandenberghe, R.E. (1992) DIST3E-program, based on the Wivel-Morup method. Laboratory of Magnetism, University of Gent, Gent, Belgium.

Vandenberghe, R.E., De Grave, E., De Geyter, G., and Landuydt, C. (1986) Characterization of goethite and hematite in a Tunisian soil profile by Mössbauer spectroscopy. *Clays and Clay Minerals,* **34,** 275–280.

Vandenberghe, R.E., De Grave, E., Bowen, L.H., and Landuydt, C. (1990) Some aspects concerning the characterization of iron oxides and hydroxides in soils and clays. *Hyperfine Interactions,* **53,** 175–196.

Walkley, A. (1946) A critical examination of a rapid method for determining organic carbon in soils. Effect of variations in digestion conditions and of inorganic soil constituents. *Soil Science,* **63,** 251–263.

E-mail of corresponding author: sacebal@criba.edu.ar

(Received 9 December 1997; accepted 8 January 2000; Ms. 97-112)